Depicting the Inner and Outer Nose: The Representation of the Nose and the Nasal Mucosa on the Human Primary Somatosensory Cortex (SI)

Mareike Gastl, Yvonne F. Brünner, Martin Wiesmann, and Jessica Freiherr*

Diagnostic and Interventional Neuroradiology, RWTH Aachen University, Aachen, Germany

Abstract: The nose is important not only for breathing, filtering air, and perceiving olfactory stimuli. Although the face and hands have been mapped, the representation of the internal and external surface of the nose on the primary somatosensory cortex (SI) is still poorly understood. To fill this gap functional magnetic resonance imaging (fMRI) was used to localize the nose and the nasal mucosa in the Brodman areas (BAs) 3b, 1, and 2 of the human postcentral gyrus (PG). Tactile stimulation during fMRI was applied via a customized pneumatically driven device to six stimulation sites: the alar wing of the nose, the lateral nasal mucosa, and the hand (serving as a reference area) on the left and right side of the body. Individual representations could be discriminated for the left and right hand, for the left nasal mucosa and left alar wing of the nose in BA 3b and BA 1 by comparing mean activation maxima and Euclidean distances. Right-sided nasal conditions and conditions in BA 2 could further be separated by different Euclidean distances. Regarding the alar wing of the nose, the results concurred with the classic sensory homunculus proposed by Penfield and colleagues. The nasal mucosa was not only determined an individual and bilateral representation, its position on the somatosensory cortex is also situated closer to the caudal end of the PG compared to that of the alar wing of the nose and the hand. As SI is commonly activated during the perception of odors, these findings underscore the importance of the knowledge of the representation of the nasal mucosa on the primary somatosensory cortex, especially for interpretation of results of functional imaging studies about the sense of smell. *Hum Brain Mapp 35:4751–4766, 2014.* © 2014 Wiley Periodicals, Inc.

Key words: primary somatosensory cortex (SI); nasal mucosa; fMRI; somatotopy; somatosensory stimulation; homunculus; olfaction

INTRODUCTION

The clarification of somatotopy in the primary somatosensory cortex (SI) of humans has passed distinct milestones since the turn of the 20th century. After Brodman (1909) created different maps for the cerebral cortex of humans, monkeys and other species and divided the human cortex into 52 cytoarchitectonic areas, Penfield and Boldrey (1937) and Penfield and Rasmussen (1950) pioneered neuroanatomical research by providing evidence for a somatotopic representation of the human body in SI. Designing a somatosensory map of the human body in SI, they called this map "somatosensory homunculus." Using

Contract grant sponsor: START program of the Medical Faculty of RWTH Aachen University.

*Correspondence to: Dr. Jessica Freiherr, Diagnostic and Interventional Neuroradiology, RWTH Aachen University, Pauwelsstr. 30, D-52074 Aachen, Germany.
E-mail: jfreiherr@ukaachen.de

Received for publication 26 November 2013; Revised 1 February 2014; Accepted 5 March 2014.

DOI 10.1002/hbm.22509
Published online 21 March 2014 in Wiley Online Library (wileyonlinelibrary.com).

electrical stimulation during neurosurgery of patients, Penfield and colleagues further discovered that the feet, the hands, and the oral area—parts of the body that are considered of high somatosensory impact—are represented in much larger areas of SI than other body parts. Moreover, Kolb and Wishaw (2003) revealed that the more important somatosensory information from a certain part of the body to a species is, the larger the area it occupies on the somatosensory cortex and the larger the density of receptors in those peripheral body parts is. All of the former and more recent studies shared a common goal: to establish an anatomical organization for the yet not entirely mapped structure of the human brain in particular, for the primary somatosensory cortex.

Somatosensory information of tactile stimulation of the human face is processed by the trigeminal nerve mediating information to its somatotopically organized nuclear complex in the medulla oblongata. From here, second-order neurons project to the contralateral thalamus through two major peripheral pathways: the dorsal column system that relays impulses for touch perception and proprioception as well as the anterolateral system that conveys nociception and temperature perception. Purely tactile stimulation of the skin is supposed to be transmitted through the dorsal column system. Information from both systems is further mediated through the contralateral ventrobasal thalamus to SI in the postcentral gyrus (PG) of the contralateral hemisphere and other cortical areas such as the secondary somatosensory cortex (SII). Evidence for an involvement of ipsilateral activation of SI and SII after tactile stimulation has recently been provided (Eickhoff et al., 2008; Kopietz et al., 2009).

SI is anatomically located on the PG and is subdivided into Brodman areas (BAs) 3b/a, 1, and 2, whereas BAs 3b/a are located on the rostral part of the PG, BA 1, and BA 2 are found on the top and caudal part, respectively. Brodman area 3a receives deep muscle sensory input, while BA 3b identifies slow neural conduction of the skin, BA 1 detects fast neural conduction of the skin. In addition, BA 2 represents activation of joints and pressure perception. Penfield and colleagues based their somatosensory homunculus on the entire PG. However, there is proof that each Brodman area in humans consists of its own homunculus (Kolb and Wishaw, 2003). Therefore, recent studies about somatosensory representation focussed on the subdivions of the PG (Eickhoff et al., 2008; Nelson and Chen, 2008; Martuzzi et al., 2014). Nguyen et al. (2005) further demonstrated a somatotopic organization of SII including three distinct areas in the parietal operculum: the parietal ventral area, a more posterior area 2, and the ventral somatosensory area (parts of BAs 40 and 43; Iwamura, 1998; Kolb and Wishaw, 2003).

While the representation of the face (Lin et al., 2010) and hands (Martuzzi et al., 2014) on the primary somatosensory cortex have already been described, the extent and nature of the mapping of the internal and external surface of the nose remain poorly understood. Somatosensory stimulation of the nasal mucosa is recorded by nasal branches of the ophthalmical (V1) and maxillary part (V2) of the trigeminal nerve in the whole nasal cavity. The original map drawn by Penfield and Boldrey (1937) indicates that the nose is represented in a very small area based on its macroanatomical relation between forehead and chin. To our knowledge, although Penfield and colleagues tried to locate the outside of the nose, they never mapped the nasal mucosa. Since those early studies, the position of the nose and the nasal mucosa on the primary somatosensory cortex of humans has not been verified using functional magnetic resonance imaging (fMRI).

Because of the functional and evolutionary relation of the nasal mucosa to the pharynx, it has since been hypothesized that the nasal mucosa is represented closer to the pharynx than to the outside of the nose (Morris, 1988). By assuming the tongue and the pharynx are anatomically localized at the caudal end of the PG (Soros et al., 2008), the location of the nasal mucosa would be expected in this region as well. Although findings of a previous study support the idea of an individual representation of the nasal mucosa in the homunculus (May, 2011), the study was hampered by various limitations: First, despite separate homunculi, the analysis was carried out only for the entire PG. Second, the subjects had to stimulate their nose manually with a Teflon® tubing nosepiece placed inside or outside their nose. This probably led to concomitant activation of the primary somatosensory cortex due to hand movements, activation of the motor cortex as well as activation of diverse other areas.

Thus, the current study aims to investigate the representation of the nose, in particular of the nasal mucosa, in the different BAs of the primary somatosensory cortex by using fMRI. To address the limitations of the aforementioned study, the current investigation utilizes a customized pneumatically driven device and uses the hand as reference area to ensure that only areas corresponding to the tactile stimulation of the nose and the nasal mucosa are evoked.

MATERIALS AND METHODS

Participants

The study was conducted in accordance with the Declaration of Helsinki and approved by the Ethics Committee at the University Hospital Aachen. Twenty-three healthy human subjects with neither history of neurological disorders nor of illnesses related to the respiratory tract gave their written informed consent. Seven subjects thereof were excluded from the study because of agoraphobia, extrinsic metallic parts in their body, anatomical brain variances, extensive head movement, and technical problems. This resulted in a final inclusion of sixteen subjects [10 females and 6 males, age range: 22–26 years, M = 23.69 years, standard deviation (SD) = 1.30 years]. As the lateralization of somatosensory processing is dominant in the

left cortical hemisphere, representing the right side of the body (Lin et al., 2010), self-reported right-handedness of the subjects was confirmed with the help of the laterality coefficient (M = 99.52, SD = 2.18, range 90–100; Oldfield, 1971).

Stimulation Device

A pneumatically driven device for tactile stimulation was customized in cooperation with the Interdisciplinary Center for Clinical Research (IZKF) Aachen and the E.ON Energy Research Center of RWTH Aachen University. The device consisted of six lines of 8 m-long Teflon® tubing leading through the waveguide of the MRI scanner. The six lines of tubing were divided into three pairs of two lines each. Each pair of tubing was connected to the two ends of a double acting, full-plastic, pneumatic-cylinder (Type 1108; PSK Ingenieursgesellschaft mbH, Erfurt, Germany). A pressure pump (Rietschle/Thomas, Sheboygan, Wisconsin) generated compressed air (approximate pressure of 5 bar), which extended and retracted the plastic piston rod of the cylinder. A gear rack was attached to the piston rod moving a gear wheel in order to translate the longitudinal movement of the piston rod into a rotation of one of the three plastic sticks. The end of each stick was covered with a Teflon® nosepiece (outer diameter = 25 mm, length = 2 cm; see Fig. 1). A rotation frequency of 1.67 Hz was chosen to potentially activate Merkel cell mechanoreceptors in the epidermis of the skin (Klinke and Silbernagel, 2003) leading to 35 turns in each stimulation block. For times of rest, a pressure control valve was interposed in the Teflon® tubing system to minimize airflow accumulation. The PC program terminal 1.9b bray (version 1.9b 20040204) was employed to synchronize the trigger signal of the MRI scanner with tactile stimulation and to control one of the three possible stimulation sites. Thus, the MRI trigger signal initiated a sequence of electrical impulses sent to a microcontroller (ATmega 16; Atmel, San Jose, CA), which itself led the stimulation impulses to a valve island (Bürkert 8640; Ingelfingen, Germany). The valve island represented the cutting point between the electrical impact and the air pressure for the tubes.

A plastic frame was mounted onto the scanner table to fixate the stimulus device while still enabling individual adjustment of the position of the Teflon pieces by a lateral movement mechanism. Additionally, the plastic sticks were covered with flexible tubes allowing for an adjustment of the nosepieces to the subjects' individual anatomy in a second way. The device was tested in 10 pilot subjects and confirmed as MRI-safe for tactile stimulation. No interferences during data acquisition could be detected.

Functional Magnetic Resonance Imaging

Participants were placed in a supine position and asked to keep their eyes closed so as to avoid any movement.

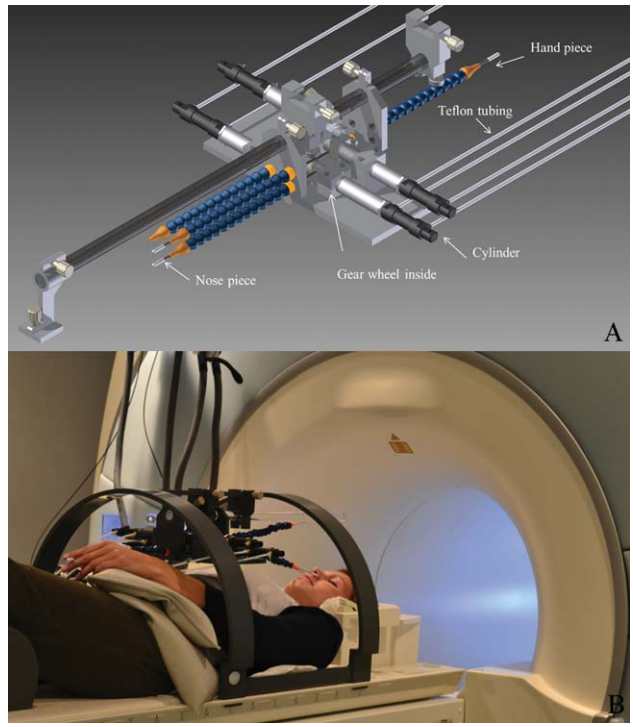

Figure 1.
(**A**) Scheme of the pneumatically driven device. The Teflon® tubing forwards the air pressure to the cylinder that moves back and forth. The gear wheel translates the longitudinal movement into a rotation of the Teflon® pieces that are applied to the stimulation sites (HL/HR, NOL/NOR, and NIL/NIR). (**B**) Positioning of the machine in the MRI scanner. The three Teflon® pieces are adjusted to the stimulation sites. The arch displays the device mounting of the machine onto the scanner table. HL/HR: hand left/right, NOL/NOR: nose outside left/right, and NIL/NIR: nose inside left/right.

Two sessions of the experiment were carried out during one experimental run. During Session A, the right alar wing of the nose (NOR), the left lateral wall of the nasal mucosa (NIL), as well as the left middle and index finger on the distal interphalangeal joint (HL) were stimulated. During Session B, the opposite side of each area was stimulated (NOL, NIR, and HR). A block design was chosen and the order of Sessions A and B was counterbalanced across subjects. Because of technical problems, 2 of the 23 subjects had to be rescanned for one session, but were still included in the cohort of sixteen subjects whose data was considered for data analysis. Since the localization of the fingers on the homunculus had already been revealed, this area was used as a reference for later analyses (Nelson and Chen, 2008; Martuzzi et al., 2014).

Each session consisted of 27 cycles of a 21s-stimulation block followed by a 21s-baseline block. The order of cycles was pseudorandomized. Stimulation blocks for each side were repeated nine times during one session. Due to the

large inter-individual variance of tactile perception threshold values and to control for habituation effects, participants rated the intensity of the stimulation for each stimulation site on a scale from 1 (not perceivable) to 10 (strong intensity) for the beginning and the end of each stimulation session (Park et al., 2001). In cases where subjects provided a rating of 10, they were separately asked whether or not they rated the stimulation as painful.

Images were acquired on a 3.0-T Trio TIM system (Siemens, Erlangen, Germany) using a 12-channel head matrix coil (Siemens) and gradient echo planar imaging (EPI), T2*-weighted sequence [47 slices of 2.5 mm thickness ensuring whole brain coverage, matrix size = 64 × 64 with field of view (FOV) = 240 mm × 240 mm, repetition time (TR) = 2,500 ms, time to echo (TE) = 22 ms, voxel size = 3.8 mm × 3.8 mm, flip angle = 70°, no parallel imaging]. Slices were oriented along the ACPC line based on a sagittal localizer image. A total of 465 functional scans per session was acquired. Each session lasted a total of 19.37 min and was followed by a gradient-echo sequence (adjusted volume of EPI sequence, TE 1 = 4.5 ms, TE 2 = 6.96 ms) to adjust for geometric distortion during analysis of the functional data. A Magnetization Prepared Rapid Gradient Echo (MPRage) structural scan [slice thickness = 1 mm, FOV = 250 mm × 250 mm, inversion time (TI) = 900 ms, TR = 1,900 ms, TE = 2.52 ms, voxel size = 1 mm × 1 mm, flip angle = 9°, no parallel imaging] was also acquired.

Statistical Analyses of the Behavioral Data

The perceptual ratings of the tactile stimulation were analyzed with a repeated-measures analysis of variance (ANOVA) in SPSS 20.0 (SPSS, Chicago, IL) with the within-subject factors "time" and "stimulation site." Mauchly's test for interaction was used to test the assumption of sphericity. If being violated, degrees of freedom were corrected using the Greenhouse–Geisser method. *P*-values below 0.05 were considered significant. An individual subject's perceptual ratings of the intensity ratings for the beginning and the end of each stimulation session were averaged and used as covariates during the analysis of the fMRI data.

fMRI Analyses

The fMRI data was analyzed using statistical parametric mapping software (SPM8; Wellcome Trust Centre for Neuroimaging, University College London, UK; Friston et al., 1994). First, the anatomical landmark of the anterior commissure on the anatomical image was used to reorient the anatomical image and all functional images with regard to zero within the Montreal Neurological Institute (MNI) space. For correcting geometric distortions, the gradient-echo field data was submitted to the Fieldmap toolbox implemented in SPM8, to create voxel displacement maps (VDMs; Jezzard, 2012). The VDMs were further applied to the functional scans which were then unwarped and motion-corrected by realigning each scan to the first scan of each series (Friston et al., 1995). Afterward, the individual anatomical scan of each subject was co-registered to the respective functional scans. By using the Bayesian rule, the probability of each voxel of the anatomical image volume belonging to a certain tissue type was assessed during segmentation (Ashburner and Friston, 2000). For one subject, the bias-corrected anatomical pattern of the first segmentation step was used as a template for another segmentation process as technical problems during the first segmentation step had occurred. All functional scans were then spatially normalized onto the standard brain template of the MNI resulting in 3 mm × 3 mm × 3 mm voxels for the functional image volumes and 1 mm × 1 mm × 1 mm voxels for the anatomical image volume (Friston et al., 1995). Preprocessing was completed by using an isotropic Gaussian kernel of 8-mm full width at half maximum for smoothing and thereby reducing the low frequency signal fluctuations in order to improve the signal-to-noise ratio.

For single-subject analysis, a block design was modeled using a boxcar function convolved with a canonical hemodynamic response function (hrf) in the context of the general linear model (Friston et al., 1995) with regressors corresponding to the onset times of the stimulation blocks during each of the six conditions. The six realignment parameters as well as the calculated mean intensity ratings of the stimulation were included as covariates of no interest. Statistical parametric maps were generated to contrast each of the conditions against baseline.

For group-level inference, a mixed-effects GLM was implemented with the factor "subjects" as random-effects factor and the factor "stimulation site" as fixed-effects factor. A main effect was set to analyze brain activation during the different stimulation conditions. Implicit anatomical regions of interest (ROIs) masks for BAs 3b, 1, and 2 of both hemispheres were defined with the help of guidelines for somatotopic mapping proposed by other cytoarchitectonic studies (Geyer et al., 1999, 2000; Grefkes et al., 2001) as implemented in the Anatomy toolbox for SPM (Eickhoff et al., 2005, 2007). In the Anatomy toolbox, the activation map of each condition as a result of the group-level analysis was masked with the defined ROIs ($P < 0.05$ FWE-corrected). For BA 2, the NOL and NIL conditions showed no activation by using the FWE-correction. Thus, an uncorrected P value of <0.01 was considered. Within those ROIs, six search coordinates for each BA were extracted for the contralateral site and two search coordinates for NIL and NIR for the ipsilateral site by choosing the center of mass (CoM) of the activation clusters with the highest number of voxels. Furthermore, the data was evaluated with respect to the individual first-level analyses. Therefore, a sphere of 5 mm was created around the eight search coordinates for each ROI and was combined with the anatomical ROIs for the BAs 3b, 1, and 2 using Marsbar in SPM (MRC Cognition and Brain

Sciences Unit, Cambridge, UK; Brett et al., 2002) as has been accomplished in other studies (Beisteiner et al., 2001; Eickhoff et al., 2008; Hétu et al., 2011; Ma et al., 2010; Nadel et al., 2013; Yoncheva et al., 2010). This was done to ensure that the sphere was only localized in a particular BA. For each subject, the new ROIs were applied to the statistical parametric maps for each stimulation site at a threshold of $P < 0.05$ (uncorrected for whole-brain comparison) using the Anatomy toolbox. Only coordinates with the highest correlated activation maximum and highest probability for the subregion were selected to account for statistical analysis. In addition to local activation maxima, cluster volumes of the activation maxima of the different conditions were extracted.

Statistical analysis encompassed two approaches to assess somatotopy in SI. First, the individual contralateral activation maxima were entered for the left or right BAs in individual repeated-measures ANOVAs in SPSS 20.0 with the two within-subject factors "stimulation site" (H, NO, and NI) and "coordinates" (x, y, and z). Second, the Euclidean distances in three-dimensional space were calculated between each of the conditions of one hemisphere. Distribution of the data was tested using Shapiro-Wilk tests. Significant differences in localizations and distances were then tested using the t-test for paired-samples for parametric data or the Wilcoxon signed-rank test for nonparametric data. P values were considered significant at $P < 0.05$.

Afterward, activation maxima were tested for differences in BAs 3b, 1, and 2. Therefore, repeated-measures ANOVAs with the two within-subjects factors "coordinates" and "BA" were calculated. Cluster volumes were entered into repeated-measures ANOVAs with the within-subjects factors "hemisphere" (right or left) or "BA" to test for cluster volume differences between the right- and left-sided conditions or between the different BAs. Another repeated-measure ANOVA was calculated with the two within-subjects factors "hemisphere" (ipsi- or contralateral) and "BA" to test for significances between ipsi- and contralateral activation maxima. t-Tests for parametric and Wilcoxon signed-rank tests for nonparametric data were subsequently computed. Again, P values were considered significant at $P < 0.05$.

Furthermore, a Matlab function that accessed Marsbar (MRC Cognition and Brain Sciences Unit, Cambridge, UK; Brett et al., 2002) was implemented to calculate the change in the BOLD signal in each of the 5-mm ROIs for the time of the stimulation. A rationale for this calculation is to compare BOLD signals between the different stimulation conditions and to proof that there had been no habituation to the stimulation. The BOLD response was averaged across the nine repetitions that had been established for each of the six stimulation conditions. One stimulation block lasted 21 s; however, activation periods were extended for 6 s after the end of the stimulation. Measuring points were set in accordance to the TR of 2.5 s, leading to 11 mean values for each condition. The mean response was calculated by considering activation of each subject on a single-subject level.

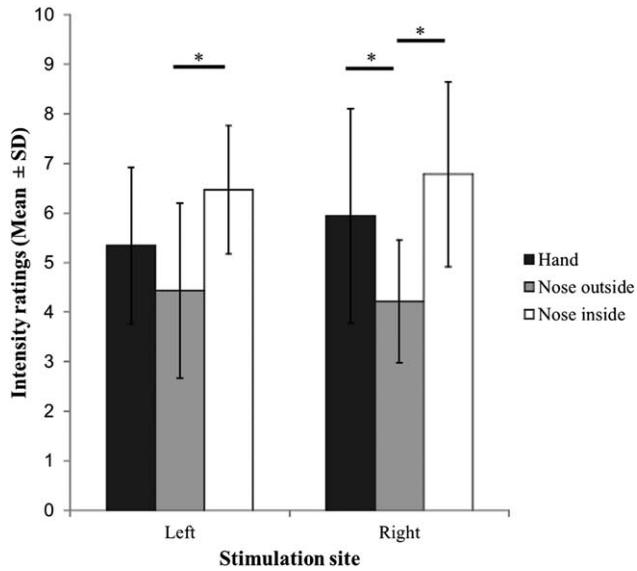

Figure 2.
Mean and standard deviation values of the perceived stimulation intensities for the six conditions. No significant difference could be detected for the stimulation at the beginning versus the end of the scanning session in a repeated-measure ANOVA in SPSS. *Pair-wise t-tests ($P < 0.05$).

RESULTS

Intensity Ratings

Ratings of perceived intensity of the stimulation were not significantly affected over time, [$F(1,15) = 2.37$, $P = 0.15$], thereby indicating that subjects did not adapt to the stimulation. For different stimulation sites, a significantly different perception of the stimulation was detected [$F(5,75) = 11.68$, $P < 0.001$]. Post hoc pair-wise t-tests showed a significant difference between the ratings of NIL versus NOL ($P = 0.011$), NIR versus NOR ($P < 0.001$), and HR versus NOR ($P = 0.007$; Fig. 2). Stimulation at NIL was rated as more intense than NOL (NIL: $M = 6.47$, SD = 1.30, range = 3–8; NOL: $M = 4.44$, SD = 1.77, range = 2–7.5, and HL: $M = 5.34$, SD = 1.58, range = 3–8). For the right-sided conditions, NIR and HR showed no significant difference, but both were more intense in comparison to NOR (NIR: $M = 6.78$, SD = 1.86, range = 3–9.5, HR: $M = 5.94$, SD = 2.16, range = 3–10, and NOR: $M = 4.22$, SD = 1.24, range = 2–7). No painful activation was reported after the rating of the highest stimulus intensity. No interaction effect between time and stimulation site was observed [$F(3.2,48.3) = 1.30$, $P = 0.285$].

Somatotopy in the PG

The mixed-model analysis for group-level inferences revealed contralateral activation in the masks of BAs 3b, 1, and 2 in each of the six contrasts following tactile

TABLE I. Search coordinates displayed by centers of mass (CoM) in MNI space in BAs 3b, 1, and 2, $P < 0.05$ FWE-corrected or $P < 0.01$ uncorrected for whole-brain comparison

	BA 3b			BA 1			BA 2		
	x	*y*	*z*	*x*	*y*	*z*	*x*	*y*	Z
HL	43	−27	53	50	−24	56	49	−30	53
NOL	56	−13	41	55	−17	50	51	−27	53
NIL	59	−11	32	63	−12	36	58	−19	37
HR	−46	−25	50	−52	−22	51	−48	−31	51
NOR	−52	−18	42	−58	−16	42	−57	−19	37
NIR	−54	−15	38	−59	−16	40	−58	−18	35

The coordinates were found by applying the ROIs of BA 3b, 1, and 2 to the different conditions on the second-level analysis. BA: Brodman area, HL/HR: hand left/right, NOL/NOR: nose outside left/right, and NIL/NIR: nose inside left/right.

TABLE II. Ipsilateral and contralateral CoMs for the stimulation of the lateral nasal mucosa in BAs 3b, 1, and 2

	BA 3b			BA 1			BA 2		
	x	*y*	*z*	*x*	*y*	*z*	*x*	*y*	Z
NIL_contra	59	−11	32	63	−12	36	58	−19	37
NIL_ipsi	−56	−14	36	−61	−14	38	−58	−18	35
NIR_contra	−54	−15	38	−59	−16	40	−58	−18	35
NIR_ipsi	58	−14	37	61	−14	39	—	—	—

Ipsilateral ROIs were found as SI-ROI and sub-ROIs on both hemispheres. CoM: center of mass, PG: postcentral gyrus, BA: Brodman area, contra: contralateral, ipsi: ipsilateral, and NIL/NIR: nose inside left/right.

stimulation ($P < 0.05$, FWE-corrected for whole-brain comparison; Fig. 3) and in BA 2 for the conditions NOL and NIL ($P < 0.01$, uncorrected for whole-brain comparison). Table I presents the CoMs of the individual ROIs, displaying the search coordinates for the single-subject analyses. Since the anatomical masks consisted of both the ipsilateral and contralateral hemispheres, an ipsilateral activation of the primary somatosensory cortex could be detected for only the right and left nasal mucosa (NIR/NIL) at a threshold of $P < 0.05$ (FWE-corrected for whole-brain comparison) with the exception of NIR in BA 2. It was observed that the *x*-, *y*-, and *z*-coordinates for the ipsilateral activation were close to the coordinates on the contralateral side: For BA 3b an ipsilateral representation for NIL was found in 11 of the 16 subjects at $x = -56$, $y = -14$, and $z = 36$ (in comparison: NIR_contra = −54, −15, 38). NIR revealed an ipsilateral activation in 8 of the 16 subjects (NIR_ipsi = 58, −14, 37, in comparison: NIL_contra = 59, −11, 32; Table II). Occurrences for BA 1 and 2 paralleled occurrences for BA 3b and are displayed with mean values and SDs in Table III. Comparison of cluster volumes of the activation maxima between the ipsilateral and contralateral sites yielded no significant differences.

Contralateral activation was found in BA 3b for the left and right hand in 13 of the 16 subjects. For the left alar wing of the nose, 9 of the 16 subjects exhibited activation maxima and for the right alar wing of the nose 11 of the 16 subjects revealed activation maxima for the left and 8 for the right lateral wall of the nasal mucosa. Although occurrences in BA 1 showed similar numbers, they were less prominent for BA 2 (see Table IV). Calculated were

TABLE III. Mean values (±SD) in MNI space and occurrences of the ipsilateral activation maxima in BA 3b, 1, and 2, $P < 0.05$ (uncorrected for whole brain comparison)

	Occ.	*x*	*y*	z
BA 3b				
NIL_ipsi	11	−56.18 ± 1.40	−17.09 ± 2.02	37.55 ± 1.21
NIR_ipsi	8	58.88 ± 1.55	−12.25 ± 2.66	38.13 ± 1.55
BA 1				
NIL_ipsi	12	−60.75 ± 1.86	−16.75 ± 2.50	38.00 ± 2.00
NIR_ipsi	9	62.00 ± 1.50	−13.33 ± 3.16	39.67 ± 1.00
BA 2				
NIL_ipsi	12	−58.50 ± 2.39	−16.75 ± 1.36	34.00 ± 0.00
NIR_ipsi	–	–	–	–

Activation maxima were selected on the subjects' first-level analysis. BA: Brodman area, NIL/NIR: nose inside left/right, and Occ.: occurences.

TABLE IV. Number of subjects with activation maxima found in contralateral SI during single-subject analysis in a group of sixteen subjects ($P < 0.05$ uncorrected for whole-brain comparison)

	BA 3b	BA 1	BA 2
HL	13	16	12
NOL	9	7	6
NIL	12	13	5
HR	13	14	9
NOR	11	9	8
NIR	8	13	12

HL/HR: hand left/right, NOL/NOR: nose outside left/right, and NIL/NIR: nose inside left/right.

the mean values and SDs of only the activation maxima with the highest t-value and probability to be in that particular region (Table V). The mean probabilities for activation maxima and their clusters for a specific localization are listed in Table VI.

A spatial organization of the six stimulation sites in all BAs was observed after the mean values had been calculated. The hand is represented in a more medial and superior position than the nose. Comparing the alar wing of the nose with the nasal mucosa, the nasal mucosa is located more lateral and inferior than the alar wing, except for the left nasal conditions in BA 2 (Figs. 3–6). Thus, the results indicate a somatotopy on the hand- and nose-level.

Comparison of the MNI coordinates confirms the idea of a somatotopic organization and reveals that the stimulation conditions are separable in the single axes. There is evidence for a significant dissociation between the three different conditions on the left side in all three axes for BA 3b [main effect "stimulation site": $F(2,10) = 16.52$, $P = 0.01$; main effect "coordinates": $F(2,10) = 4855.93$, $P < 0.001$; interaction effect: $F(4,20) = 275.0$, $P < 0.001$, HL vs. NOL: $P = 0.016$ for all axes, $n = 7$, HL vs. NIL: $P = 0.004$ for all axes, $n = 10$, NOL vs. NIL: $P = 0.01$ for x-axis, $P = 0.023$ for y-axis, $P = 0.011$ for z-axis, $n = 8$]. Significance in locations in the right-sided conditions could be established for HR versus NOR ($P = 0.008$ for x-axis, $P = 0.007$ for y- and z-direction, $n = 9$), and HR versus NIR [$P = 0.016$ for all axes, $n = 7$; main effect "stimulation site": $F(2,8) = 34.75$, $P < 0.001$; main effect "coordinates": $F(2,8) = 3795.68$, $P < 0.001$; interaction effect: $F(4,16) = 40.83$, $P < 0.001$].

As a second approach to show separable localizations, the Euclidean distances between each condition of one side were tested for differences from zero (one-sample t-test). Figure 4 shows the averaged Euclidean distances for

TABLE VI. Mean values (±SD) of the activation maxima in MNI space in BA 3b, 1, and 2, $P < 0.05$ (uncorrected)

	x	y	z
BA 3b			
HL	44.31 ± 1.32	−25.69 ± 1.80	54.54 ± 1.13
NOL	55.33 ± 1.58	−14.67 ± 1.58	41.00 ± 2.60
NIL	60.25 ± 0.87	−11.50 ± 1.57	32.50 ± 2.39
HR	−45.92 ± 2.84	−25.46 ± 1.66	51.08 ± 1.44
NOR	−53.18 ± 1.94	−17.09 ± 1.51	41.09 ± 3.36
NIR	−55.50 ± 1.60	−16.00 ± 2.27	38.50 ± 1.60
BA 1			
HL	50.19 ± 2.32	−23.25 ± 1.84	57.31 ± 1.25
NOL	57.00 ± 0.00	−16.43 ± 1.13	48.57 ± 3.21
NIL	62.77 ± 1.92	−11.38 ± 1.56	38.15 ± 3.36
HR	−52.93 ± 1.49	−22.86 ± 2.18	52.43 ± 2.31
NOR	−58.33 ± 1.58	−16.33 ± 2.35	42.00 ± 3.35
NIR	−59.54 ± 1.13	−16.54 ± 2.07	40.23 ± 3.11
BA 2			
HL	49.92 ± 1.44	−28.67 ± 1.23	54.50 ± 1.17
NOL	51.00 ± 2.45	−28.00 ± 2.45	53.29 ± 2.36
NIL	59.00 ± 1.41	−22.00 ± 0.00	39.20 ± 1.30
HR	−49.11 ± 1.83	−31.00 ± 2.12	51.78 ± 0.67
NOR	−57.00 ± 0.00	−10.00 ± 0.00	34.00 ± 0.00
NIR	−59.00 ± 1.48	−16.75 ± 1.36	34.00 ± 0.00

Activation maxima were selected on the subjects' first-level analysis. BA: Brodman area, HL/HR: hand left/right, NOL/NOR: nose outside left/right, and NIL/NIR: nose inside left/right.

TABLE V. Mean probabilities (in %, ±SD) for the location of clusters and their activation maxima in BA 3b, 1, and 2 during first-level analysis

	BA 3b		BA 1		BA 2	
	AM	Cluster	AM	Cluster	AM	Cluster
HL	83.08 ±12.51	94.77 ± 2.84	85.63 ± 8.14	85.18 ± 5.42	84.17 ± 5.15	92.93 ± 2.57
NOL	55.56 ± 8.82	84.42 ± 4.27	77.14 ±13.80	60.33 ± 7.52	83.33 ± 5.16	90.17 ± 2.25
NIL	53.33 ± 8.80	92.92 ± 2.69	64.62 ± 7.76	72.32 ± 5.48	40.00 ± 0.00	75.58 ± 12.43
HR	63.85 ± 6.50	78.9 ± 11.47	77.14 ± 7.26	70.30 ± 10.75	74.77 ± 5.27	79.80 ± 3.42
NOR	61.82 ± 10.79	79.51 ± 9.20	54.00 ± 15.78	58.03 ± 4.79	30.00 ± 0.00	26.10 ± 10.18
NIR	57.50 ± 8.86	80.40 ± 3.23	51.54 ± 8.99	51.61 ± 5.12	25.83 ± 9.00	28.25 ± 5.52

AM: activation maxima, BA: Brodman area, HL/HR: hand left/right, NOL/NOR: nose outside left/right, and NIL/NIR: nose inside left/right.

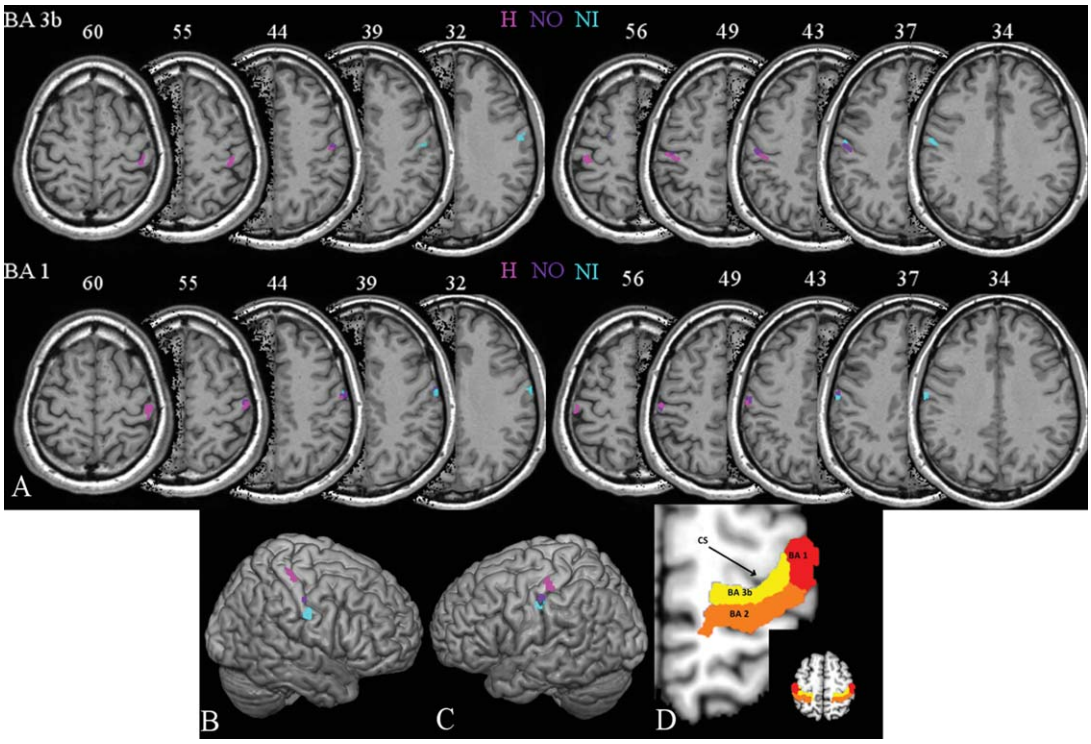

Figure 3.

Results for the nasal and hand mapping procedure. In (**A**), group-level clusters are displayed in axial slices in BAs 3b and 1. The first column displays stimulation conditions on the left side of the body, whereas the second column represents the right side. The color code is displayed in the middle of the figure and will be maintained for Figures 4–8. The maps of BA 3b of one representative subject are displayed on the right cortical surface in (**B**), and on the left cortical surface in (**C**). The right cortex represents the left part of the body and vice versa. In (**D**), the different ROIs of the PG for the single-subject analyses are displayed in an axial slice. As anatomical reference, the CS is indicated on the slice. BA: Brodman area; H: hand; NO: nose outside; NI: nose inside; PG: postcentral gyrus; and CS: central sulcus.

BA 3b. It was observed that the Euclidean distances of the activation maxima were significantly different from zero ($P < 0.05$). Pairs that are separable include HL versus NOL separated by 21.2 ± 3.3 mm ($P < 0.001$), HL versus NIL separated by 30.9 ± 1.7 mm ($P < 0.001$), NOL versus NIL separated by 10.1 ± 3.8 mm ($P < 0.001$), HR versus NOR separated by 15.2 ± 3.2 mm ($P < 0.001$), HR versus NIR separated by 17.6 ± 3.0 mm ($P < 0.001$), and NOR versus NIR separated by 4.9 ± 1.9 mm ($P = 0.004$).

Activation patterns in BA 1 paralleled the results of BA 3b [left: main effect "stimulation site": $F(2,12) = 11.71$, $P = 0.002$; main effect "coordinates": $F(2,12) = 7640.22$, $P < 0.001$; interaction effect: $F(2,10) = 130.16$, $P < 0.001$; right: main effect "stimulation side": $F(2,16) = 25.62$, $P < 0.001$; main effect "coordinates": $F(1,9) = 7844.76$, $P < 0.001$; interaction effect: $F(4,32) = 53.61$, $P < 0.001$]. Contrasts separable in medial to lateral dimension (x-axis) include HL versus NOL ($P = 0.015$, $n = 7$), NOL versus NIL ($P = 0.014$, $n = 7$), and HR versus NIR ($P = 0.002$, $n = 11$). In anterior to posterior direction (y-axis), they include HL versus NOL ($P = 0.017$), HL versus NIL ($P = 0.001$, value for x- and z-dimension equal, $n = 13$), NOL versus NIL ($P = 0.014$), HR versus NOR ($P = 0.011$, value for x- and z-dimension equal, $n = 8$), and HR versus NIR ($P = 0.003$). Separable locations for inferior to superior dimension (z-axis) comprise HL versus NOL, NOL versus NIL ($P = 0.017$), and HR versus NIR ($P = 0.003$). P-values for testing the three-dimensional distances remained significant. They were 14.6 ± 3.0 mm for HL-NOL ($P < 0.001$), 26.2 ± 3.7 mm for HL-NIL ($P < 0.001$), 13.2 ± 4.0 mm for NOL-NIL ($P < 0.001$), 14.0 ± 4.5 mm for HR-NOR ($P < 0.001$), 15.0 ± 3.6 mm for HR-NIR ($P < 0.001$), and 4.9 ± 3.1 mm for NOR-NIR ($P = 0.016$; Fig. 5).

In BA 2, the results were less clear [left: main effect "stimulation site": n.s.; main effect "coordinates": $F(2,6) = 10063.897$, $P < 0.001$; interaction effect: $F(4,12) = 58.18$, $P < 0.001$; right: main effect "stimulation site": $F(2,8) = 67.82$, $P < 0.001$; main effect "coordinates": $F(2,8) = 36748.632$, $P < 0.001$; interaction effect: $F(4,16) = 276.29$, $P < 0.001$]. Only activation maxima of HL versus NIL ($P = 0.039$ for all dimensions, $n = 5$), HR versus NOR ($P = 0.024$ for x- and y-dimensions, $P = 0.014$ for z-dimension, $n = 6$), HR versus NIR ($P = 0.017$ for x-, $P = 0.016$ for y-

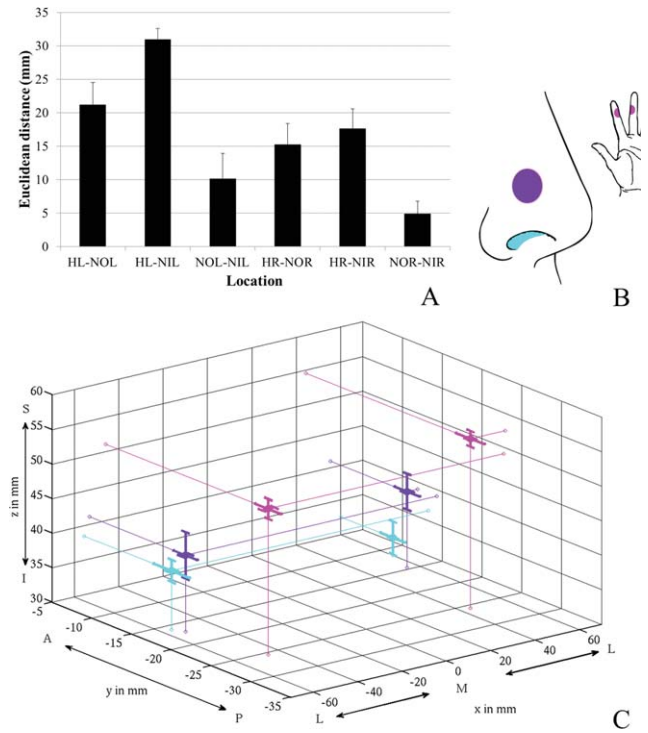

Figure 4.

Results for BA 3b in the first-level analysis of each volunteer. (**A**) Euclidean distances (in mm) were calculated between the activation maxima of the single conditions. Error bars represent the standard deviations of the mean. All distances were tested to be significantly different from zero in parametric one-sample *t*-tests. (**B**) Different colors indicate the three different stimulation sites. (**C**) Mean coordinates (±SD) for the different locations. The coordinates were found by applying a 5-mm ROI to the CoM of an activation cluster as search coordinate at a threshold of $P < 0.05$ uncorrected for whole-brain volume. Activation maxima with the highest probability to be in PG were selected. PG: postcentral gyrus; CoM: center of mass; HL/HR: hand left/right, NOL/NOR: nose outside left/right; and NIL/NIR: nose inside left/right.

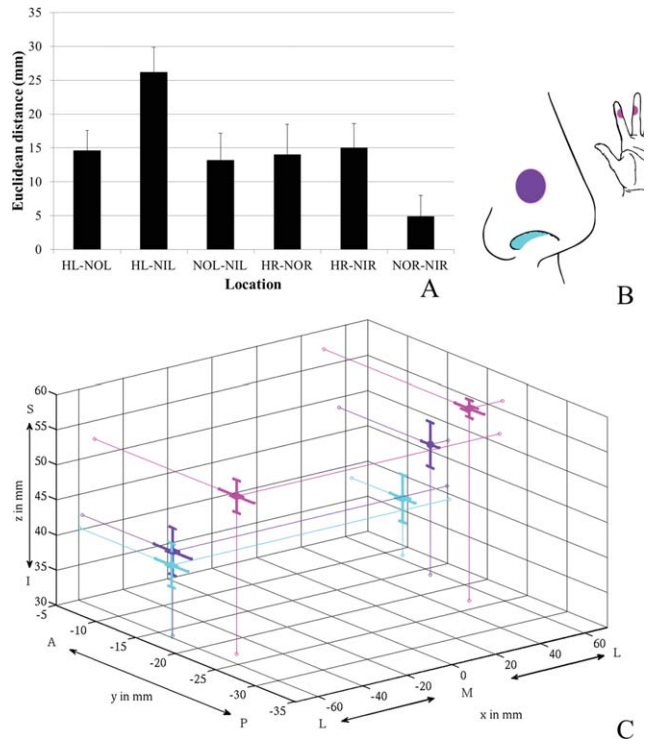

Figure 5.

Results for BA 1 in the first-level analysis of each volunteer. (**A**) Euclidean distances (in mm) were calculated between the activation maxima of the single conditions. Error bars represent the standard deviations of the mean. All distances were tested to be significantly different from zero during parametric one-sample *t*-tests. (**B**) Different colors indicate the three different stimulation sites. (**C**) Mean coordinates (±SD) for the different locations. The coordinates were found by applying a 5-mm ROI to the CoM of an activation cluster as search coordinate at a threshold of $P < 0.05$ uncorrected for whole-brain volume. Activation maxima with the highest probability to be in PG were selected. PG: postcentral gyrus; CoM: center of mass; HL/HR: hand left/right; NOL/NOR: nose outside left/right; and NIL/NIR: nose inside left/right.

and $P = 0.008$ for *z*-dimension, $n = 7$), and NOR versus NIR ($P = 0.046$ for *x*-dimension, $n = 6$) differed significantly regarding their localization. Statistical tendencies were shown in HL versus NOL ($P = 0.068$ for *x*-dimension, $n = 6$) and NOL versus NIL ($P = 0.068$ for *x*- and *z*-, $P = 0.066$ for *y*-dimension, $n = 5$). Results from Euclidean distance analyses further suggested separable localizations, $P = 0.002$ for HL versus NOL (4.48 ± 1.81 mm), $P < 0.001$ for HL versus NIL (19.30 ± 1.47 mm), $P = 0.002$ for NOL versus NIL (17.27 ± 3.11 mm), $P = 0.026$ for HR versus NOR (24.40 ± 1.32 mm), $P < 0.001$ for HR versus NIR (24.99 ± 1.64 mm), and $P = 0.025$ for NOR versus NIR (2.5 ± 1.22 mm; Fig. 6).

To summarize the results for BA 3b and 1, somatotopy is demonstrated for both sides of the hand, the alar wing of the nose and the nasal mucosa of the left side of the nose when testing activation maxima. No separable locations could be discerned between nasal mucosa and alar wing of the right side of the nose. In contrast to the lack of somatotopic organization for the right side of the nose, the one-sample Wilcoxon signed-rank test of the Euclidean distances showed significant separable representations for all conditions. Regarding BA 2, the hands can still be distinguished for their localization except for comparing to the alar wing of the nose; different stimulation sites of the nose are not clearly distinguished, but distances still suggest individual localizations in three-dimensional space.

Cluster volumes of all stimulation conditions except NOL were tested distinctly in their size when compared between the different BAs [HR: $F(2,20) = 32.10$, $P < 0.001$,

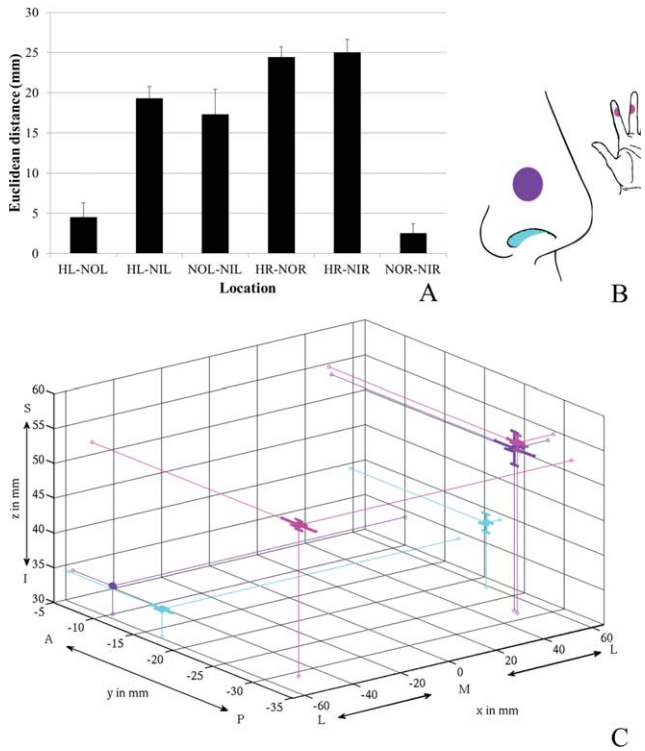

Figure 6.

Results for BA 2 in the first-level analysis of each volunteer. (**A**) Euclidean distances (in mm) were calculated between the activation maxima of the single conditions. Error bars represent the standard deviations of the mean. All distances were tested to be significantly different from zero during parametric one-sample *t*-tests. (**B**) Different colors indicate the three different stimulation sites. (**C**) Mean coordinates (±SD) for the different locations. The coordinates were found by applying a 5-mm ROI to the CoM of an activation cluster as search coordinate at a threshold of $P < 0.05$ uncorrected for whole-brain volume. Activation maxima with the highest probability to be in PG were selected. PG: postcentral gyrus; CoM: center of mass; HL/HR: hand left/right; NOL/NOR: nose outside left/right; and NIL/NIR: nose inside left/right.

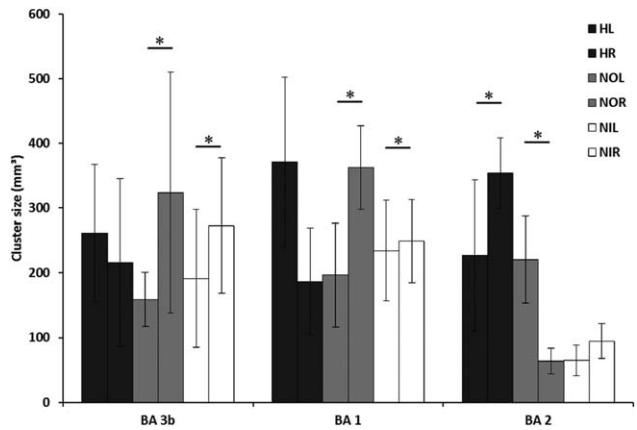

Figure 7.

Cluster volume sizes for all conditions in BAs 3b, 1, and 2. For BAs 3b and 1, cluster volumes are higher for the right side compared to the left side for the conditions NO and NI. Additional cluster volume sizes are lower for BA 2 compared to the other BAs except for HL and NOL. HL/HR: hand left/right; NOL/NOR: nose outside left/right; and NIL/NIR: nose inside left/right. *Pair-wise *t*-tests ($P < 0.05$).

NIL: $F(2,8) = 23.28$, $P < 0.001$, HR: $F(2,16) = 12.29$, $P = 0.001$, NAR: $F(2,8) = 14.57$, $P = 0.008$, NIR: $F(2,12) = 23.10$, $P < 0.001$]. During the following *t*-tests, cluster volumes for all conditions were equal upon comparison between BA 3b and 1 except from HL, but upon the respective comparison with BA 2, significant *P* values were detected except for HL: HL 3b versus 1: $P < 0.001$; 2 versus 1: $P < 0.001$; NIL 3b versus 2: $P = 0.017$; 2 versus 1: $P < 0.001$; HR 3b versus 2: $P = 0.027$; 2 versus 1: $P < 0.001$; NOR 3b versus 2: $P = 0.002$; 2 versus 1: $P = 0.001$; and NIR 3b versus 2: $P = 0.001$; 2 versus 1: $P < 0.001$. In general, cluster volumes were significantly lower in BA 2 than in BA 3b and BA 1 (Fig. 7). *t*-Tests comparing the cluster volumes of the right and left side of the body showed a significant effect for all BAs except for HL versus HR in BA 3b and 1 and NIL versus NIR in BA 2. These results indicate that the right side of the body shows greater cluster volumes for NO and NI in BA 3b and BA 1 than the left side of the body.

The BOLD response over time depicts several activation peaks during the 21s-stimulation of each condition before decreasing at the end of the stimulation (Fig. 8). All BOLD intensity change curves start at a value above zero at the beginning of the stimulation block. The hand shows the strongest BOLD response followed by the intranasal mucosa and the alar wing in all BAs. For the conditions of the nose, the average BOLD response for the right side of the body is larger than for the left side. With respect to BA 2, the results are not as clear, because BOLD responses for NIL and NOR showed an undulant shape and no clear activation peaks.

DISCUSSION

The aim of this study was to delineate the representation of the lateral nasal mucosa, the alar wing of the nose and the hand as a reference in the BAs on the primary somatosensory cortex. Using tactile stimulation with a custom-designed, pneumatically driven device, we observed a clear individual representation of the left-sided nasal conditions in BAs 3b, 1. For the right-sided conditions as well as for BA 2 different Euclidean distances still highlight a separate representation. In these representations, the hand was in a superior and more medial position than the nasal mucosa and the alar wing of the nose. In the nasal stimulation conditions, the nasal mucosa was located more lateral and inferior.

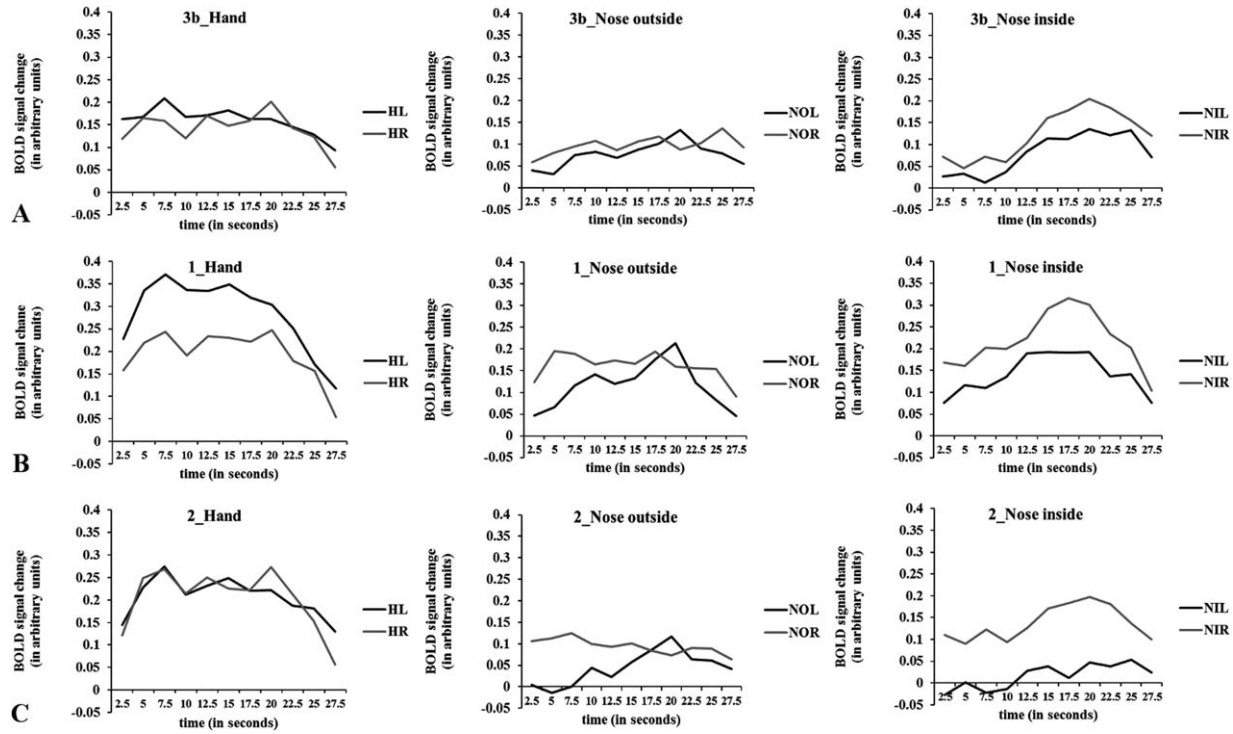

Figure 8.

Average BOLD signal change for all subjects in all conditions and repetitions. One stimulation block lasts 21s. The *x*-axes display 11 time points with regard to the TR of 2.5 s, and *y*-axes represent signal intensity change (in AU). Brodman area 3b is displayed in (**A**) followed by BA 1 (**B**) and BA 2 (**C**). Curves of the graph start at the time point of 2.5 s after stimulation. The hand shows the highest BOLD signal. The signal for the right side of the body is superior compared to the signal of the left side for the nasal conditions. There is no habituation to the stimulus, because different peaks exist. A low constant BOLD signal during baseline conditions is assumed, as the curves start above zero. BA: Brodman area, HL/HR: hand left/right, NOL/NOR: nose outside left/right, NIL/NIR: nose inside left/right.

Anatomical Localization of the Different Conditions on SI

Despite the clearly separable localizations for the left stimulation sites in BAs 3b and 1, significant representation of the right stimulation conditions was less precise in these BAs (Figs. 3–5). Only the right hand was represented individually; however, the alignment of all right-sided conditions with the hand placed more superior and the lateral wall of the nasal mucosa most inferior was still consistent.

The inclusion of only right-handed subjects may explain the lack of separate localizations on the left cortical hemisphere that represents the right side of the body. Kotecha et al. (2009) reported that the volume of the cortical activation cluster whilst stimulating the right finger was significantly larger than the activation cluster elicited by the left finger. Hence, activation clusters for the right side of the body are likely to overlap and complicate the identification of separable localizations. Other studies support these findings (Jung et al., 2008; Sörös et al., 1999; Simões et al., 2002). In addition, BOLD signal changes and cluster volumes have shown a higher response for the right nasal conditions compared to the left ones (Fig. 8).

Another indicator for a difference in both hemispheres is that functional asymmetries for the hemispheres exist in the language (Grabowska et al., 1994; Steinmetz et al., 1991) and motor systems (Rose et al., 2012; Serrien et al., 2012). Knowledge about the effect of left- and right-handedness on representation on the somatosensory cortex would have a big impact on successive studies focusing on somatotopy of SI. Further research is needed to address this issue.

For BA 2 we were not able to separate the representation of the inner and outer nose, neither for the left nor for the right side. Moreover, since fewer subjects responded to the stimulation in BA 2 (Table IV), a significant different representation of both conditions was

harder to prove during statistical analysis. Nelson et al. (2008) and Martuzzi et al. (2014) experienced the same reduced neural response in BA 2 of subjects upon applying a vibrotactile stimulation to the fingers. Given the converging input of joints and of pressure to BA 2, it is not surprising that fewer subjects responded to the stimulation. Other stimulus categories that represent the submodalities joints and pressure or, alternatively, an MRI-Scanner with a higher field strength than 3 T may be better suited to show a somatotopic organization in BA 2 (Chung et al., 2013). This is especially supported by lower cluster volumes of BA 2 and undulant plotted shapes for the changes in the BOLD signal in NIL and NOR (Fig. 8). Ferrington and Rowe (1980) further described that Pacinian corpuscles are necessary to project contralaterally into BA 2 (Francis et al., 2000; Gelnar et al., 1998) and a very high stimulation frequency of more than 50 Hz is required to activate Pacinian corpuscles (Chung et al., 2013; Ferrington and Rowe, 1980). We chose a stimulation frequency of approximately 2 Hz to potentially activate Merkel cells in the epidermis that project into BAs 3b and 1. This has been proven as a robust stimulation design in previous settings (Eickhoff et al., 2008; Kampe et al., 2000; Krubitzer, 1995).

Anatomical Localization in Comparison to Other Studies

The results of this present study concur with those of previous fMRI studies focusing on somatotopy of the hand and face in the primary somatosensory cortex. Martuzzi et al. (2014) and Nelson et al. (2008) observed the representation of the middle and index finger in BAs 3b, 1, and 2 using fMRI (i.e., $x = -44$, $z = 54$ and $x = 43$, $z = 51$ for the index and middle finger in BA 3b) and depicted them in an area close to the coordinates we established ($x = -46$, $z = 51$ in BA 3b; Francis et al., 2000; van Westen et al., 2004). Hence, the hand served as a good indicator to prove the accuracy and functionality of the present study design.

A review of the findings of Penfield and Boldrey (1937) and Penfield and Rasmussen (1950), in which they delineated the nose below the forehead and the thumb of the hand, showed consistency for the coordinates of the alar wing of the nose. More recent studies tested the representation of the face on SI (Kopietz et al., 2009; Lin et al., 2010). Here, the contrast for the cheek activated the PG at $z = 39$ and $z = 40$. Both studies agree with our findings for the representation of the alar wing of the nose ($z = 41$).

As stated previously, the nasal mucosa is located more inferior on the PG than the alar wing of the nose (NOL with $z = 41$ vs. NIL with $z = 32.5$ and NOR with $z = 41$ vs. NIR with $z = 38.5$). This extends the findings of past research by May (2011), in which a self-applied stimulus activated the following brain areas after stimulation of the two sites of the nose, NO with $z = 40$ and NI with $z = 32$. The nasal mucosa is represented more caudally than the chin (Kopietz et al., 2009) and closer to the lips, the tongue, and the pharynx on the caudal end of the PG. Fesl et al. (2003) examined the localization of the tongue in an fMRI study and reported activation to be at $z = 34$ and $z = 30$ (left: $x, y, z = -62, -6, 34$ and right: $x, y, z = 66, -6, 30$). In a second study, Miyamoto et al. (2006) found the tongue to be located at $z = 40$ ($x, y, z = -60.1, -5.2, 40.1$). Soros et al. (2008) pictured the left side of the pharynx at $z = 29$ ($x, y, z = 62, -13, 29$), whereas Blatow et al. (2007) depicted the lips at $z = 38$ (lips left: $x, y, z = 57.8, -9.29, 37.93$ and lips right $x, y, z = -58.89, -13.1, 38.05$). Compared to each of those coordinates, the nasal mucosa is represented closer to other parts of the upper airway than to the alar wing of the nose. This agrees with the anatomical and evolutionary relation in which the primary nasal cavity develops from the oral cavity with the palate displaying the horizontal border during the second month of embryonic growth. To function properly, all parts of the upper airway are linked among themselves and they feature the warming and cleaning of the inhaled air during breathing. They are covered by mucosa, whereas the outer nose consists of squamous epithelium.

The coordinates of the lateral wall of the nasal mucosa in the current study are similar to those found during a meta-analysis of functional imaging studies. Albrecht et al. (2010) analyzed the findings of nine fMRI and PET studies during which the intranasal trigeminal system was stimulated by carbon dioxide (CO_2), representing a painful stimulus. In this meta-analysis, an activation of the PG was found at $x = 49$, $y = -11$ and $z = 25$. Both nociception and somatosensory perception are features of the trigeminal nerve, and it is not surprising that the results are reflected in the current study.

Euclidean Distances

The Euclidean distances between the different conditions observed here highlight what was reported previously. Distances in each condition and region were proved to be significantly different from zero, underscoring the separate localizations of the hand, the alar wing of the nose, and the nasal mucosa. The distances between the hand and the alar wing of the nose are consequently lower than the distances between the hand and the nasal mucosa (i.e., 21.2 mm for HL-NOL vs. 39.9 mm for HL-NIL in BA 3b; Figs. 4–6). Thus, the nasal mucosa is located farther away from the hand and closer to the caudal end of the PG and the upper airway structures. Upon applying the formula for the Euclidean distances to compare the current findings to those of Fesl et al. (2003), the distance between the tongue and the alar wing of the nose is twice the respective distance to the nasal mucosa (i.e., 12.3 mm for tongue to NOL and 6.0 mm for tongue to NIL in BA 3b). Finally, it is noteworthy that the measurement of the Euclidean distances is a common

approach that was used in several studies in the past (van Westen et al., 2004; Nelson and Chen, 2008; Martuzzi et al., 2012). Although it is an approximation function to depict relations of coordinates in the brain, unfortunately, it cannot cover the 3D-structure of the brain. In future studies, another way to calculate differences in the cortical surface in form of 2D-projections is a function called ISOVIEW that was first introduced by Erb et al. (1999) and Lotze et al. (2000).

BOLD Response

In this current study, the BOLD response was plotted for the single conditions as a function of time to depict the course of the blood flow during stimulation (Fig. 8). This was done to compare intensities and the time courses of the BOLD signal in the different conditions and to proof that there had been no habitation to the stimulation. Surprisingly, the BOLD response showed hemodynamic response even before the beginning of the stimulation conditions as has been found by Graham et al. (2001). Indeed, Fransson (2005) found out that there is a low frequency BOLD signal of 0.012–0.1 Hz in the resting brain and Zhang and Ding (2010) reported the mu rhythm, an ongoing neural activity in human SI that is characterized of field potential oscillations in the 7–13 Hz range. However, spontaneous fluctuations may not explain the prestimulus BOLD response satisfactorily. Another reason might be the noise level of the prestimulus interval such as the fact that the nosepieces were adapted to the stimulation sides throughout the whole session and only started rotating during the stimulation blocks. Further, there is evidence that tactile expectations modulate prestimulus activation in SI (Carlsson et al., 2000). Although the subjects did not know the exact length of the stimulation and resting blocks, they probably expected stimulation after some time of rest. This is especially the case since we did not use a jittered length of the resting blocks.

The change in the BOLD responses during the 21-s stimulation showed several peaks before decreasing at the end of the stimulation. This can help to explain the potential shortcoming of the present study that touching one's nose from the outside is an everyday action whereas inserting a Teflon® tube into the nostril is usually less common, thereby leading to faster or slower habituation. The shapes of the BOLD responses with several peaks indicate that subjects do not adapt to the stimulation. In addition, Rankin et al. (2009) pointed out that the weaker a stimulus is, the bigger the chance for a faster habituation. We detected a significantly higher sensitivity of the nasal mucosa compared to that of the alar wing of the nose, because the stimulation of the nasal mucosa was evaluated to be more intense (Fig. 2). However, the stable intensity ratings of the stimulation of the alar wing of the nose point out that the primary somatosensory cortex might not adapt to the stimulation in a second way (Klingner et al., 2014; Popescu et al., 2010).

As mentioned earlier, the BOLD response can also help to explain the lack of anatomical differentiation between the right nasal mucosa and the right alar wing of the nose, because the blood oxygenation level indicates higher responses for the right-sided nasal conditions compared to those of the left.

Bilateral Activation in SI

Although bilateral activation of the secondary somatosensory cortex (SII) after tactile stimulation is considered to be a prerequisite (Blatow et al., 2007; Ferretti et al., 2004; Naito et al., 2005; Young et al., 2004), there is ample evidence that the primary somatosensory cortex (SI) possesses transcallosal connections for some parts of the body. Transcallosal projections of SI have already been revealed in non-human primates (Burton and Fabri, 1995; Iwamura et al., 2002; Lipton et al., 2006). Eickhoff et al. (2008) reported a bilateral hemispheric activation after stimulation of the human face and the trunk in BAs 3b, 1, and 2 of humans. There was no bilateral activation of the hand in those areas except for BA 2 that is supposed to have evolved from increased manual capabilities. Similar findings have been published about the face (Blatow et al., 2007; Ferretti et al., 2004; Iannilli et al., 2008; Naito et al., 2005; Young et al., 2004) and the trunk (Fabri et al., 2005, 2006; Itomi et al., 2000). A transcallosal activation due to stimulation of the buccal mucosa, the tongue, and the lips has been reported in 2008 (Tamura et al., 2008). Extending upon this issue, the results of the current study also reflect the lack of bihemispheric activation after tactile stimulation of the fingers. We found a bilateral activation of the nasal mucosa for BAs 3b, 1, and 2. The ipsilateral activation maxima were established in the same orientation as the contralateral maxima on the other side (Tables II and III). Their cluster sizes are even equal to the cluster size of the contralateral site, thereby indicating an equally strong activation in both hemispheres. As we chose to stimulate the lateral wall of the nasal mucosa, it is not likely to find a simultaneous stimulation of both nasal cavities at once, although this possibility exists. Despite previous findings of a bilateral representation of the face, the alar wing of the nose lacked a bihemispheric activation and challenges the importance of the outer skin of the nose.

In short, our findings underline the individual and close localization of the nasal mucosa and the mucosa of the upper airway in the caudal end of the PG on the right hemisphere. Nevertheless, the nasal mucosa is represented closer to the mucosa of the upper airway than the alar wing in the left hemisphere. This highlights the importance of the somatosensory impact of the nasal mucosa for sensory perception of our environment. In addition to its role during breathing and filtering of the inhaled air, the second important function of the nose is chemosensory

perception. Apart from its importance for food consumption, smelling comprises many functions of the body such as warning a person against danger and for hygiene. Previous studies have shown the activation of the primary somatosensory cortex during odor perception (Boyle et al., 2007; Iannilli et al., 2013; Kobal, 2003; Simonyan et al., 2007; Sobel et al., 1998) or the activation of olfactory brain areas during chemosensory perception of the nasal mucosa (Cain and Murphy, 1980; Iannilli et al., 2008). Hence, activation of the nasal mucosa would be valuable for information processing and the assessment of an olfactory stimulus. The warning function of the sense of smell is an example: sensory bihemispheric integration helps the body to respond adequately by performing a flight reaction. Yet what is still unknown is the exact connection between the olfactory pathway and the somatosensory system, which should be the subject of further research.

CONCLUSION

This study has shown a newly developed and pneumatically driven device to precisely and noninvasively activate areas corresponding to the lateral wall of the nasal mucosa, the alar wing of the nose and the middle and index finger. This method enables the individual somatotopic localization of the left nasal mucosa in BAs 3b and 1 of the PG. The localization of the nasal mucosa is closer to the localization of the pharynx as compared to the representation of the alar wing of the nose. Somatotopic variability is found to be less prominent in right-sided conditions and BA 2, but different Euclidean distances still highlight distinct localizations. In BAs 3b and 1, the representation of the inner and outer part of the nose is organized in a somatotopic order in which the nasal mucosa is located more inferiorly and laterally. Also observed is an ipsilateral activation of the SI for the right and left nasal mucosa (NIR/NIL). Consequently, this study has helped to further clarify the somatotopy of the nose and nasal mucosa in the primary somatosensory cortex of humans.

ACKNOWLEDGMENTS

We are grateful to Florian Kölzer from the Brain Imaging Facility at the Interdisciplinary Center for Clinical Research (IZKF) Aachen and Felix Adler at the E.ON Energy Research Center RWTH Aachen for their technical expertise during the design and implementation of the custom-made tactile stimulation device. Furthermore, we wish to express our gratitude to Georg Eder, Erika Söndgen, and Angelika Becker from the Brain Imaging Facility at the Interdisciplinary Center for Clinical Research (IZKF) Aachen for their technical assistance during scanning sessions. We also want to thank Christina Regenbogen now at Karolinska Institute, Stockholm, Sweden and André Schüppen and David Weyer from the Brain Imaging Facility at the Interdisciplinary Center for Clinical Research (IZKF) Aachen for their technical support during fMRI data analysis with Matlab and SPM8.

REFERENCES

Albrecht J, Kopietz R, Frasnelli J, Wiesmann M, Hummel T, Lundström JN (2010): The neuronal correlates of intranasal trigeminal function-an ALE meta-analysis of human functional brain imaging data. Brain Res Rev 62:183–196.

Ashburner J, Friston KJ (2000): Voxel-based morphometry--the methods. Neuroimage 11:805–821.

Beisteiner R, Windischberger C, Lanzenberger R, Edward V, Cunnington R, Erdler M, Gartus A, Streibl B, Moser E, Deecke L (2001): Finger somatotopy in human motor cortex. Neuroimage 13:1016–1026.

Blatow M, Nennig E, Durst A, Sartor K, Stippich C (2007): fMRI reflects functional connectivity of human somatosensory cortex. Neuroimage 37:927–936.

Boyle JA, Frasnelli J, Gerber J, Heinke M, Hummel T (2007): Cross-modal integration of intranasal stimuli: A functional magnetic resonance imaging study. Neuroscience 149:223–231.

Brett M, Anton J, Valabregue R, Poline J (2002): Region of interest analysis using an SPM toolbox. Neuroimage 16(2).

Brodman K (1909): Vergleichende Lokalisationslehre der Grosshirnrinde: In ihren Prinzipien dargestellt auf Grund des Zellenbaues. Leipzig: J.A. Barth.

Burton H, Fabri M (1995): Ipsilateral intracortical connections of physiologically defined cutaneous representations in areas 3b and 1 of macaque monkeys: Projections in the vicinity of the central sulcus. J Comp Neurol 355:508–538.

Cain WS, Murphy CL (1980): Interaction between chemoreceptive modalities of odour and irritation. Nature 284:255–257.

Carlsson K, Petrovic P, Skare S, Petersson KM, Ingvar M (2000): Tickling expectations: Neural processing in anticipation of a sensory stimulus. J Cogn Neurosci 12:691–703.

Chung YG, Kim J, Han SW, Kim H-S, Choi MH, Chung S-C, Park J-Y, Kim S-P (2013): Frequency-dependent patterns of somatosensory cortical responses to vibrotactile stimulation in humans: A fMRI study. Brain Res 1504:47–57.

Eickhoff SB, Grefkes C, Fink GR, Zilles K (2008): Functional lateralization of face, hand, and trunk representation in anatomically defined human somatosensory areas. Cereb Cortex 18: 2820–2830.

Eickhoff SB, Paus T, Caspers S, Grosbras MH, Evans AC, Zilles K, Amunts K (2007): Assignment of functional activations to probabilistic cytoarchitectonic areas revisited. Neuroimage 36: 511–521.

Eickhoff SB, Stephan KE, Mohlberg H, Grefkes C, Fink GR, Amunts K, Zilles K (2005): A new SPM toolbox for combining probabilistic cytoarchitectonic maps and functional imaging data. Neuroimage 25:1325–1335.

Erb M, Lotze M, Grodd W (1999): ISOVIEW: Two-dimensional display of cortical fMRI activation. Neuroimage S32–S32.

Fabri M, Polonara G, Mascioli G, Paggi A, Salvolini U, Manzoni T (2006): Contribution of the corpus callosum to bilateral representation of the trunk midline in the human brain: An fMRI study of callosotomized patients. Eur J Neurosci 23:3139–3148.

Fabri M, Polonara G, Salvolini U, Manzoni T (2005): Bilateral cortical representation of the trunk midline in human first somatic sensory area. Hum Brain Mapp 25:287–296.

Ferretti A, Del Gratta C, Babiloni C, Caulo M, Arienzo D, Tartaro A, Rossini PM, Romani GL (2004): Functional topography of the secondary somatosensory cortex for nonpainful and painful stimulation of median and tibial nerve: An fMRI study. Neuroimage 23:1217–1225.

Ferrington DG, Rowe M (1980): Differential contributions to coding of cutaneous vibratory information by cortical somatosensory areas I and II. J Neurophysiol 43:310–331.

Fesl G, Moriggl B, Schmid U., Naidich T., Herholz K, Yousry T. (2003): Inferior central sulcus: Variations of anatomy and function on the example of the motor tongue area. Neuroimage 20: 601–610.

Francis ST, Kelly EF, Bowtell R, Dunseath WJ, Folger SE, McGlone F (2000): fMRI of the responses to vibratory stimulation of digit tips. Neuroimage 11:188–202.

Fransson P (2005): Spontaneous low-frequency BOLD signal fluctuations: An fMRI investigation of the resting-state default mode of brain function hypothesis. Hum Brain Mapp 26:15–29.

Friston KJ, Ashburner J, Frith CD, Poline J-B, Heather JD, Frackowiak RSJ (1995): Spatial registration and normalization of images. Hum Brain Mapp 3:165–189.

Friston KJ, Holmes AP, Worsley KJ, Poline J-P, Frith CD, Frackowiak RSJ (1994): Statistical parametric maps in functional imaging: A general linear approach. Hum Brain Mapp 2: 189–210.

Gelnar PA, Krauss BR, Szeverenyi NM, Apkarian A V (1998): Fingertip representation in the human somatosensory cortex: An fMRI study. Neuroimage 7:261–283.

Geyer S, Schleicher A, Zilles K (1999): Areas 3a, 3b, and 1 of human primary somatosensory cortex. Neuroimage 10:63–83.

Geyer S, Schormann T, Mohlberg H, Zilles K (2000): Areas 3a, 3b, and 1 of human primary somatosensory cortex. Part 2. Spatial normalization to standard anatomical space. Neuroimage 11: 684–696.

Grabowska A, Herman A, Nowicka A, Szatkowska I, Szelag E (1994): Individual differences in the functional asymmetry of the human brain. Acta Neurobiol Exp (Wars) 54:155–162.

Graham SJ, Staines WR, Nelson A, Plewes DB, McIlroy WE (2001): New devices to deliver somatosensory stimuli during functional MRI. Magn Reson Med 46:436–442.

Grefkes C, Geyer S, Schormann T, Roland P, Zilles K (2001): Human somatosensory area 2: Observer-independent cytoarchitectonic mapping, interindividual variability, and population map. Neuroimage 14:617–631.

Hétu S, Mercier C, Eugène F, Michon P-E, Jackson PL (2011): Modulation of brain activity during action observation: Influence of perspective, transitivity and meaningfulness. PLoS One 6:e24728.

Iannilli E, Del Gratta C, Gerber JC, Romani GL, Hummel T (2008): Trigeminal activation using chemical, electrical, and mechanical stimuli. Pain 139:376–388.

Iannilli E, Wiens S, Arshamian A, Seo H-S (2013): A spatiotemporal comparison between olfactory and trigeminal event-related potentials. Neuroimage 77:254–261.

Itomi K, Kakigi R, Maeda K, Hoshiyama M (2000): Dermatome versus homunculus; detailed topography of the primary somatosensory cortex following trunk stimulation. Clin Neurophysiol 111:405–412.

Iwamura Y (1998): Hierarchical somatosensory processing. Curr Opin Neurobiol 8:522–528.

Iwamura Y, Tanaka M, Iriki A, Taoka M, Toda T (2002): Processing of tactile and kinesthetic signals from bilateral sides of the body in the postcentral gyrus of awake monkeys. Behav Brain Res 135:185–190.

Jezzard P (2012): Correction of geometric distortion in fMRI data. Neuroimage 62:648–651.

Jung P, Baumgärtner U, Magerl W, Treede R-D (2008): Hemispheric asymmetry of hand representation in human primary somatosensory cortex and handedness. Clin Neurophysiol 119: 2579–2586.

Kampe KK, Jones RA, Auer DP (2000): Frequency dependence of the functional MRI response after electrical median nerve stimulation. Hum Brain Mapp 9:106–114.

Klingner CM, Hasler C, Brodoehl S, Witte OW (2014): Excitatory and inhibitory mechanisms underlying somatosensory habituation. Hum Brain Mapp 35(1): 152-160.

Klinke R, Silbernagel S (2003): Lehrbuch der Physiologie, 4. korrigierte Auflage. Stuttgart: Georg Thieme Verlag.

Kobal G (2003): Electrophysiological measurement of olfactory function. Neurol Dis Ther 57:229–250.

Kolb, B., Wishaw IQ (2003): Fundamentals of Human Neuropsychology, 5th ed. New York: Worth Publishers.

Kopietz R, Sakar V, Albrecht J, Kleemann AM, Schopf V, Yousry I, Linn J, Fesl G, Wiesmann M (2009): Activation of primary and secondary somatosensory regions following tactile stimulation of the face. Klin Neuroradiol 19:135–144.

Kotecha R, Xiang J, Wang Y, Huo X, Hemasilpin N, Fujiwara H, Rose D, deGrauw T (2009): Time, frequency and volumetric differences of high-frequency neuromagnetic oscillation between left and right somatosensory cortices. Int J Psychophysiol 72:102–110.

Krubitzer L (1995): The organization of neocortex in mammals: Are species differences really so different? Trends Neurosci 18: 408–417.

Lin CC, Sun YN, Huang CI, Yu CY, Ju MS (2010): Cortical activation by tactile stimulation to face and anterior neck areas: An fMRI study with three analytic methods. Hum Brain Mapp 31: 1876–1885.

Lipton ML, Fu K-MG, Branch CA, Schroeder CE (2006): Ipsilateral hand input to area 3b revealed by converging hemodynamic and electrophysiological analyses in macaque monkeys. J Neurosci 26:180–185.

Lotze M, Erb M, Flor H, Huelsmann E, Godde B, Grodd W (2000): fMRI evaluation of somatotopic representation in human primary motor cortex. Neuroimage 11:473–481.

Ma L, Wang B, Narayana S, Hazeltine E, Chen X, Robin DA, Fox PT, Xiong J (2010): Changes in regional activity are accompanied with changes in inter-regional connectivity during 4 weeks motor learning. Brain Res 1318:64–76.

Martuzzi R, van der Zwaag W, Farthouat J, Gruetter R, Blanke O (2014): Human finger somatotopy in areas 3b, 1, and 2: A 7 T fMRI study using a natural stimulus. Hum Brain Mapp 35: 213-226.

May J (2011): Repräsentation der Nase und der Nasenschleimhaut auf dem menschlichen somatosensorischen Kortex; eine funktionelle Magnetresonanzstudie.

Miyamoto JJ, Honda M, Saito DN, Okada T, Ono T, Ohyama K, Sadato N (2006): The representation of the human oral area in the somatosensory cortex: A functional MRI study. Cereb Cortex 16:669–675.

Morris IR (1988): Functional anatomy of the upper airway. Emerg Med Clin North Am 6:639–669.

Nadel L, Hoscheidt S, Ryan LR (2013): Spatial cognition and the hippocampus: The anterior-posterior axis. J Cogn Neurosci 25: 22–28.

Naito E, Roland P, Grefkes C, Choi HJ, Eickhoff SB, Geyer S, Zilles K, Ehrsson HH (2005): Dominance of the right hemisphere and role of area 2 in human kinesthesia. J Neurophysiol 93:1020–1034.

Nelson AJ, Chen R (2008): Digit somatotopy within cortical areas of the postcentral gyrus in humans. Cereb Cortex 18:2341–2351.

Nguyen BT, Inui K, Hoshiyama M, Nakata H, Kakigi R (2005): Face representation in the human secondary somatosensory cortex. Clin Neurophysiol 116:1247–1253.

Oldfield RC (1971): The assessment and analysis of handedness: The Edinburgh inventory. Neuropsychologia 9:97–113.

Park R, Wallace MS, Schulteis G (2001): Relative sensitivity to alfentanil and reliability of current perception threshold vs von Frey tactile stimulation and thermal sensory testing. J Peripher Nerv Syst 6:232–240.

Penfield W, Boldrey E (1937): Somatic motor and sensory representation in the cerebral cortex of man as studied by electrical stimulation. Brain A J Neurol.

Penfield W, Rasmussen T (1950): The Cerebral Cortex of Man; a Clinical Study of Localization of Function. New York: The Macmillan Company.

Popescu M, Barlow S, Popescu E-A, Estep ME, Venkatesan L, Auer ET, Brooks WM (2010): Cutaneous stimulation of the digits and lips evokes responses with different adaptation patterns in primary somatosensory cortex. Neuroimage 52:1477–1486.

Rankin CH, Abrams T, Barry RJ, Bhatnagar S, Clayton DF, Colombo J, Coppola G, Geyer MA, Glanzman DL, Marsland S, McSweeney FK, Wilson DA, Wu C-F, Thompson RF (2009): Habituation revisited: An updated and revised description of the behavioral characteristics of habituation. Neurobiol Learn Mem 92:135–138.

Rose S, Rowland T, Pannek K, Baumann F, Coulthard A, McCombe P, Henderson R (2012): Structural hemispheric asymmetries in the human precentral gyrus hand representation. Neuroscience 210:211–221.

Serrien DJ, Sovijärvi-Spapé MM, Farnsworth B (2012): Bimanual control processes and the role of handedness. Neuropsychology 26:802–807.

Simões C, Alary F, Forss N, Hari R (2002): Left-hemisphere-dominant SII activation after bilateral median nerve stimulation. Neuroimage 15:686–690.

Simonyan K, Saad ZS, Loucks TMJ, Poletto CJ, Ludlow CL (2007): Functional neuroanatomy of human voluntary cough and sniff production. Neuroimage 37:401–409.

Sobel N, Prabhakaran V, Desmond JE, Glover GH, Goode RL, Sullivan E V, Gabrieli JD (1998): Sniffing and smelling: Separate subsystems in the human olfactory cortex. Nature 392: 282–286.

Sörös P, Knecht S, Imai T, Gürtler S, Lütkenhöner B, Ringelstein EB, Henningsen H (1999): Cortical asymmetries of the human somatosensory hand representation in right- and left-handers. Neurosci Lett 271:89–92.

Soros P, Lalone E, Smith R, Stevens T, Theurer J, Menon RS, Martin RE (2008): Functional MRI of oropharyngeal air-pulse stimulation. Neuroscience 153:1300–1308.

Steinmetz H, Volkmann J, Jäncke L, Freund HJ (1991): Anatomical left-right asymmetry of language-related temporal cortex is different in left- and right-handers. Ann Neurol 29:315–319.

Tamura Y, Shibukawa Y, Shintani M, Kaneko Y, Ichinohe T (2008): Oral structure representation in human somatosensory cortex. Neuroimage 43:128–135.

Van Westen D, Fransson P, Olsrud J, Rosén B, Lundborg G, Larsson E-M (2004): Fingersomatotopy in area 3b: An fMRI-study. BMC Neurosci 5:28.

Yoncheva YN, Zevin JD, Maurer U, McCandliss BD (2010): Auditory selective attention to speech modulates activity in the visual word form area. Cereb Cortex 20:622–632.

Young JP, Herath P, Eickhoff SB, Choi J, Grefkes C, Zilles K, Roland PE (2004): Somatotopy and attentional modulation of the human parietal and opercular regions. J Neurosci 24:5391–5399.

Zhang Y, Ding M (2010): Detection of a weak somatosensory stimulus: Role of the prestimulus mu rhythm and its top-down modulation. J Cogn Neurosci 22:307–322.